

Effect of heating rate on the properties of silicon carbide fiber with chemical-vapor-cured polycarbosilane fiber

Tae-Eon KIM, Khos-Erdene KHISHIGBAYAR, Kwang Youn CHO*

Ceramic Fiber and Composite Materials Center, Korea Institute of Ceramic Engineering and Technology, 101, Soho-ro, Jinju-si, Gyeongsangnam-do, 660-031, R. O. Korea

Received: September 09, 2016; Revised: December 14, 2016; Accepted: January 05, 2017

© The Author(s) 2017. This article is published with open access at Springerlink.com

Abstract: Silicon carbide (SiC) fiber has recently received considerable attention as promising next-generation fiber because of its high strength at temperatures greater than 1300 °C in air. High-quality SiC fiber is primarily made through a curing and heat treatment process. In this study, the chemical vapor curing method, instead of the thermal oxidation curing method, was used to prepare cured polycarbosilane (PCS) fiber. During the high temperature heat treatment of the cured PCS fiber, varied heating rates of 10, 20, 30, and 40 °C/min were applied. Throughout the process, the fiber remained in the amorphous silicon carbide phase, and the measured tensile strength was the greatest when the oxygen content in the heat-treated fiber was low, due to the rapid heating rate. The fiber produced through this method was also found to have excellent internal oxidation properties. This fast, continuous process shows a great promise for the production of SiC fiber and the development of high-quality products.

Keywords: polycarbosilane (PCS); silicon carbide (SiC) fiber; chemical vapor curing; rapid heating rate; high temperature tensile strength

1 Introduction

Industrial technologies for fiber production have rapidly advanced over the past few decades. In the case of silicon carbide (SiC) fiber, due to its unique characteristics, such as chemical inertness, ultra-high temperature stability, high mechanical strength, and high thermal conductivity, it has been gathering particular attention as an important factor in future fiber industry growth; it is expected to dominate over carbon fiber for the future applications [1,2]. However, since the development of polycarbosilane (PCS) raw material for SiC fiber production by S. Yajima in the 1970s [3],

only minor studies have been conducted on commercialization and functional enhancement of SiC fiber [4].

Continuous SiC fiber production can be divided largely into three phases: synthesis of an organo-metallic polymer PCS precursor, fiber spinning and curing of spun fiber, and high temperature pyrolysis [5]. The curing is a sensitive process that cross-links PCS, converting the linear structure of thermoplastic polymer into thermosetting polymer under a series of reactions, including dehydrogenation and oxidation. Conventional thermal oxidation [6] and electron beam irradiation [7] methods have been used successfully for the last several decades. However, additional methods have been developed for curing of the PCS precursor, and a chemical vapor curing method using iodine to induce

* Corresponding author.
E-mail: kycho@kicet.re.kr

cross-linking at low temperatures (80–120 °C) has shown very promising results [8]. Absorption and diffusion of halogen vapor occur on the surface and interior of the PCS fiber, rapidly inducing Si–H, C–H, and Si–Si cleavage with subsequent recombination to form Si–O–Si, Si–C, and C=C bonds. The cured polymer PCS fiber also undergoes pyrolysis to produce SiO and CO gas in the heat treatment process, forming Si–C–O and Si–C bonds within the SiC fiber. Thus, the curing and heat treatment processes are important elements of the organic–inorganic transition for fabrication of SiC fiber. These processes determine the mechanical strength of SiC fiber by the amount of oxygen involved in the formation of silicon oxycarbide (SiC_xO_y) yielding beta-SiC crystals at temperatures less than 1300 °C.

William *et al.* [9] studied the relationship between the mechanical strength of fiber and oxygen content of the Si–C–O form in the SiC fiber. Fiber produced with low oxygen content shows a lower degree of pyrolysis at high temperatures (> 1600 °C). Shimoo *et al.* [10] investigated fiber curing by the electron-beam irradiation curing method and heat treatment at heating rates of 0.8, 5, and 10 °C/min. They observed that SiC fiber heat-treated at more rapid heating rates has larger beta-SiC crystallite size and shows a greater increase in tensile strength.

In this study, PCS fiber cured with halogen vapor was pyrolyzed at various heating rates to evaluate its effects on the pyrolyzed SiC fiber. It was observed that the portions of the C–H and Si–H compounds are dehydrogenated by iodine vapor curing and recombined into Si–O–Si bonds, leading to the cross-linkage within the PCS fiber. This type of fiber curing was achieved by significantly increasing heating rates in present work. Unlike other studies, the heating rates were controlled to 10, 20, 30, and 40 °C/min during the heat treatment. Through examination of the morphology, crystal structure, chemical composition, and high temperature tensile strength of fiber heat-treated in this manner, it was confirmed that oxygen content can be controlled during SiC fiber production. Furthermore, differences in diameter, determined by the fiber heating rate, were correlated to oxygen content by thermogravimetric analysis. This novel method has promise in the continuous rapid production of high-quality products as an alternative to the batch-type SiC fiber production.

2 Experimental

2.1 Fabrication of SiC fiber

Polycarbosilane (PCS, ToBeM Tech.) was used as a precursor for SiC fiber production. The characteristics of the PCS precursor were measured and summarized in Table 1. The SiC fiber was spun using a melt-spinning apparatus with single-hole spinneret. The single-hole spinneret containing the precursor, was maintained under vacuum for 1 h at 120 °C. And then, the temperature was raised to 215 °C under an argon atmosphere at 0.5 bar of pressure. Moreover, with an argon gas pressure of approximately 0.1 bar, molten PCS from the single-hole spinneret was spun at approximately 400 rpm for 15 min. The spun PCS fiber was cured under an iodine vapor atmosphere as described in our earlier work [8]; it was proceeded with 40 wt% ratio of iodine to PCS. The spun PCS fiber was loaded into the sieve, and placed in vacuum oven with an iodine concentration of 0.91 mmol/L. Subsequently, the solid iodine was induced for vaporization as further detailed in Fig. 1. The iodine vapor curing process lasted for 3 h at 120 °C for cross-linking within the PCS (heating rate: 10 °C/min) under a nitrogen atmosphere. Furthermore, the PCS fiber cured at the optimized iodine concentration was pyrolyzed with heating rates of 10, 20, 30, and 40 °C/min up to 1300 °C and maintained for 1 h at that temperature. The crystallinity, mechanical strength, and internal oxidation properties of SiC fiber were determined as a function of heating rate used for the heat treatment.

2.2 SiC fiber microstructure analysis and evaluation of fiber properties

The pyrolysis behavior of PCS fiber cured with heating rates of 10, 20, 30, and 40 °C/min under an argon atmosphere was evaluated with TGA (thermogravimetric analysis; METTLER-TOLEDO, 851e, USA) and related to the heating rate and self-yield of PCS. SiC fiber previously heat treated at the listed heating rates was exposed to 1100 °C with

Table 1 Typical properties of polycarbosilane

PCS company	Softening point (°C)	Melting point (°C)	GPC		TGA
			M _n (Da)	M _w (Da)	Ceramic yield
ToBeM Tech. (R. O. Korea)	167	197	1387	4092	52.16%

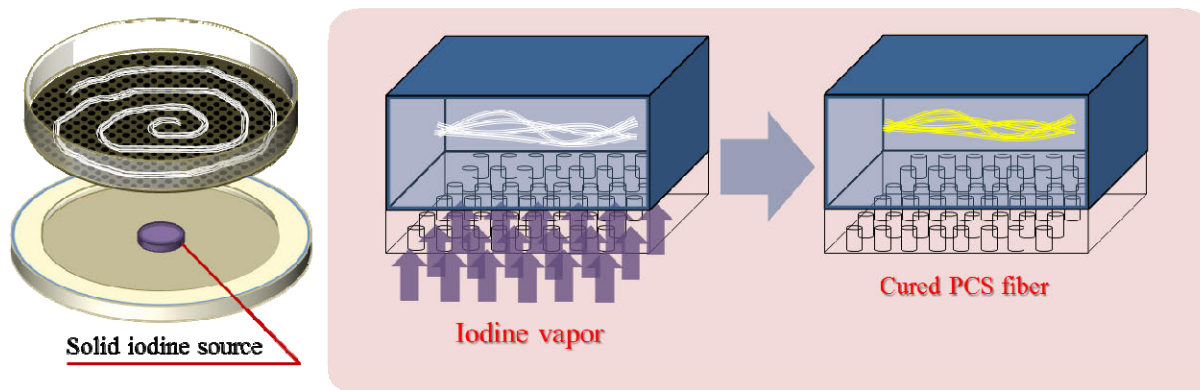


Fig. 1 Illustration of iodine vapor curing process.

heating rate of $10\text{ }^{\circ}\text{C}/\text{min}$ in air atmosphere for determination of oxidation resistance, and it maintained for 1 h at that temperature. A temperature controller (Eurothermal 9100, USA) with capillary tubes was employed to determine the softening and melting point of PCS. GPC (gel permeation chromatography; Waters, USA) with toluene (Daejung) as a solvent was used to measure the molecular weight of PCS. Functional group changes of each fiber until SiC fiber formation were measured with a potassium bromide (KBr, Daejung) pellet via FT-IR (Fourier transform-infrared spectroscopy; Jasco-4100, Japan) in range of $400\text{--}4000\text{ cm}^{-1}$ wavelength. In addition, an FE-SEM (field emission-scanning electron microscope; JSM-6700F, Japan) was used to examine the appearance and microstructure of the SiC fiber with simultaneous EDS (energy dispersive spectroscopy; AMEREK GENESIS XM2, USA) measurements. XRD (X-ray diffraction; Rigaku D/max-2500/PC, Japan) was used to analyze the structure of individual crystals of the SiC fiber. The density of heat-treated SiC fiber (for each heating rate) was obtained using an AccuPyc 1330 from Micromeritics, with helium gas. Finally, a self-induced tensile strength measurement system (load cell: UMI-G200, DACELL, R. O. Korea) was used for SiC fiber mechanical strength measurements, in which SiC fiber for each testing condition was attached to a test sheet and pulled at the speed of $0.5\text{ mm}/\text{min}$. A summary of these results is presented in the following sections.

3 Results and discussion

FT-IR spectrum analysis was performed on the PCS precursor before SiC fiber production, as shown in Fig. 2, to establish a baseline and examine changes in the

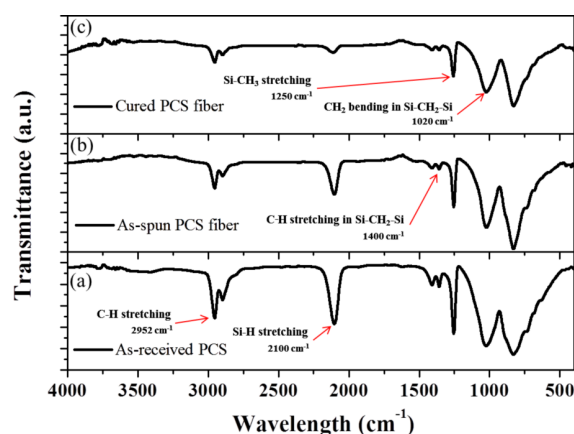


Fig. 2 FT-IR spectra of (a) as-received PCS, (b) as-spun PCS fiber, and (c) cured PCS fiber.

molecular structure of PCS. All of the raw materials, PCS, melt-spun PCS fiber, and the cured PCS fiber, were evaluated. To confirm the structure of PCS [11], stretching of C–H bonds in the PCS is verified at $2900\text{--}2950\text{ cm}^{-1}$, and the stretching of Si–H bonds is observed at 2100 cm^{-1} . Further, bending of C–H bonds in Si–CH₂–Si structure is observed at 1400 and 1360 cm^{-1} , and the stretching of the Si–CH₃ structure is confirmed at 1250 cm^{-1} . However, the melt-spun PCS fiber shows a greater decrease in Si–H and C–H bonds than PCS, and a dramatic decrease in Si–H and C–H bonds after the curing process using iodine vapor. This confirms that iodine induces dehydrogenation in Si–H and C–H bonds and creates a three-dimensional molecular structure within the PCS fiber, thereby converting PCS fiber into a thermosetting polymer [12].

Figure 3 is a simplified schematic diagram of the changes in the internal molecular structure of PCS fiber, as derived from examination of the PCS fiber after the curing process and the final heat-treated SiC fiber. The PCS is mixed structure of Si–CH₃ and Si–H bonds, with Si–CH₂–Si bonds forming the molecular backbone of

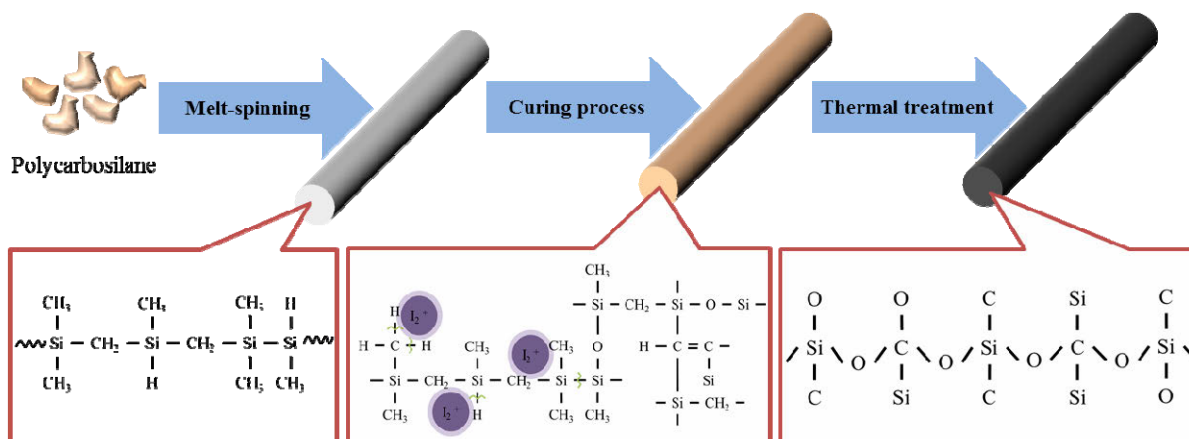


Fig. 3 Schematic illustration of conversion process for PCS to SiC fiber.

the PCS. As curing progresses, the iodine vapor causes dehydrogenation in Si–H and C–H bonds, where either oxygen adheres to the broken connection to form Si–O–Si bond or direct Si–C bonding occurs. This forms the three-dimensional structure of a thermosetting polymer type, which allows its fibrous nature to be maintained without melting even at high temperatures.

Figure 4 shows a crystal structure analysis of SiC fiber produced at each heating rate in a graphite furnace after the iodine vapor curing. The zinc blende crystal structure is observed with beta-SiC phases at 36.5° (111), 60.1° (220), and 73° (311) due to the beta-SiC phase structure of amorphous silicon oxycarbide (SiC_xO_y) [13,14]. A typical amorphous SiOC phase is observed as halo at $2\theta = 19^\circ\text{--}24^\circ$ in all the fabricated SiC fiber [15].

Figure 5 shows cross-sectional images of the produced fiber at each heating rate. Generally, smooth fiber is observed, and the overall distribution of the fiber diameter is shown in Fig. 6. The average diameter

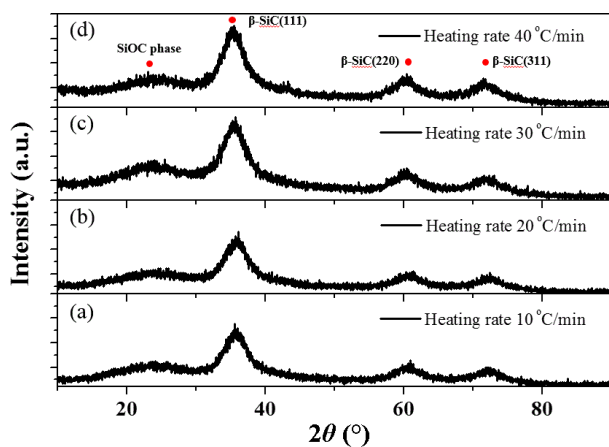


Fig. 4 XRD patterns of SiC fiber at different heating rates.

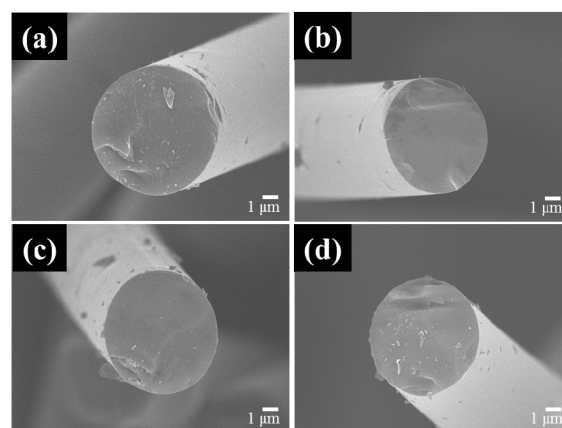


Fig. 5 Micro-morphology (cross-sectional images) of SiC fiber at different heating rates: (a) $10^\circ\text{C}/\text{min}$, (b) $20^\circ\text{C}/\text{min}$, (c) $30^\circ\text{C}/\text{min}$, and (d) $40^\circ\text{C}/\text{min}$.

is $13.735\ \mu\text{m}$ for the slowest heating rate of $10^\circ\text{C}/\text{min}$. As the heating rate is increased to 20, 30, and $40^\circ\text{C}/\text{min}$, decreases in the fiber's average diameter to 13.439, 12.607, and $11.865\ \mu\text{m}$, respectively, are observed. It is considered that the significant high degree of pyrolysis can be induced within the PCS fiber with faster heating rate during the heat treatment.

Furthermore, EDS analysis verified the elemental composition of each heat-treated fiber at different heating rates (Table 2). The overall C/Si ratio of SiC fiber is maintained at 0.6. However, a decrease in the oxygen ratio is observed with increased heating rate. For the slowest heating rate of $10^\circ\text{C}/\text{min}$, the ratio is 10.862 at%, whereas the ratio is 8.148 at% for the fastest heating rate of $40^\circ\text{C}/\text{min}$, indicating an approximately 2 at% decrease in oxygen content of the fiber during heat treatment. Therefore, it is confirmed

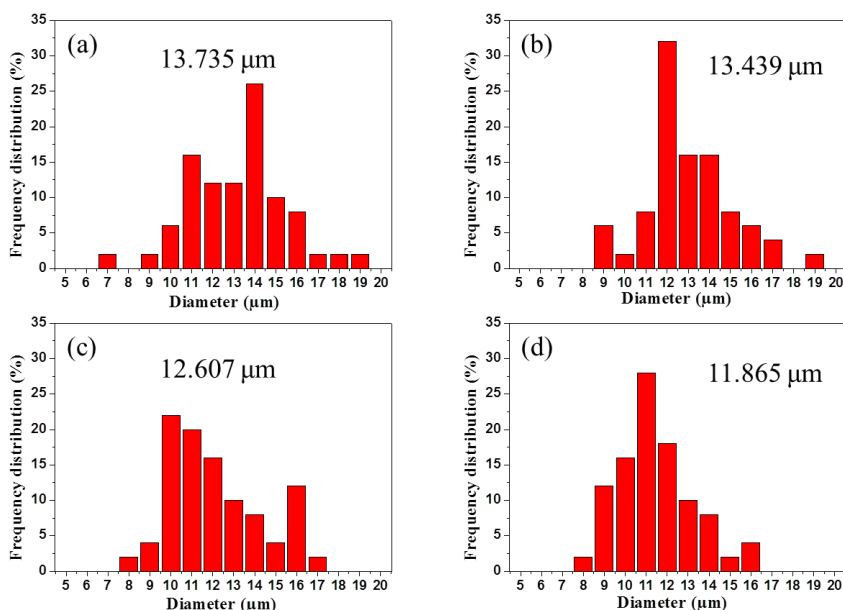


Fig. 6 Diameter distribution of SiC fiber at different heating rates: (a) 10 °C/min, (b) 20 °C/min, (c) 30 °C/min, and (d) 40 °C/min.

Table 2 Elemental composition of SiC fiber at different heating rates (Unit: at%)

Element	Heating rate			
	10 °C/min	20 °C/min	30 °C/min	40 °C/min
Si	59.968	56.850	56.236	58.658
O	10.862	10.254	8.180	8.148
C	27.306	31.184	33.434	31.220
I	1.864	1.712	2.144	1.974

that the higher heating rate of pyrolysis can hinder the oxidative reaction during the heat treatment process and it causes a small diameter of SiC fiber with low oxygen content. The density of each fiber was also measured for each heating rate (Table 3). According to the literature, the density of pure SiC crystal is 3.21 g/cm³ [3,16]. However, the densities of SiC fiber fabricated at 10, 20, 30, and 40 °C/min are 2.9438, 2.8699, 2.8531, and 2.7987 g/cm³, respectively, indicating a 4.9% decrease in density between the fastest heating rate and the slowest. The slight decrease in density is believed to be the result of shorter exposure time to high temperatures with the faster heating rate. In summary, commercially available products of Nicalon 200 (Nippon Carbon) and Tyranno LOX-M (Ube Ind.) were analyzed for comparison with SiC fiber, which consist of amorphous silicon oxycarbide. In comparison to these products, the fiber produced in this study has higher density, smaller diameter, and lower oxygen content [17].

Table 3 Density of SiC fiber at different heating rates

Density (g/cm ³)	Heating rate			
	10 °C/min	20 °C/min	30 °C/min	40 °C/min
	2.9438	2.8699	2.8531	2.7987

Accordingly, to verify the reason for the heating rate’s effect on oxygen content and diameter, weight change was analyzed by TGA, as shown in Fig. 7. When this test is performed on PCS fiber cured with iodine vapor at a heating rate of 10 °C/min, the final weight of the fiber has a yield of 79.3511% up to 1000 °C. With greater heating rates, the yield decreases to 72.634% (heating rate: 20 °C/min), 70.8832% (heating rate: 30 °C/min), and 54.9553% for a heating rate of 40 °C/min.

$SiC_xO_y(s) = SiC(s) + SiO(g) + CO(g)$ (1)
 From this, it is concluded that with faster heating rate, emission of CO or SiO gas increases, as shown in Eq. (1) [18] resulting in greater pyrolysis, greater shrinkage in the fiber shape, and reduced oxygen content due to fewer oxygen-bonded parts.

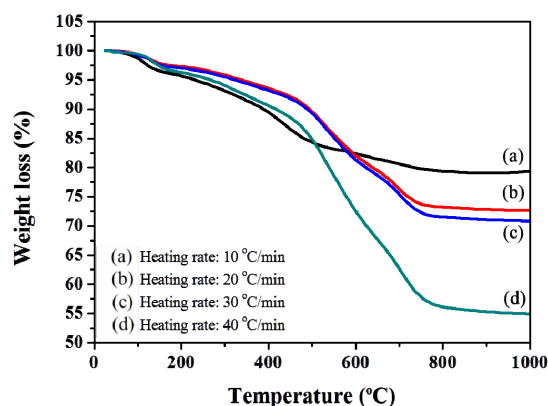


Fig. 7 TGA curves of thermal decomposed behavior for cured PCS fiber at different heating rates.

The average tensile strength and elasticity of SiC fiber produced with various heating rates is shown in Fig. 8 and Table 4. The measurements were taken at room temperature, 1000 °C, and 1400 °C, while exposed to air. A general decrease in fiber strength is observed at higher temperatures; however, SiC fiber heat-treated at heating rate of 40 °C/min, which has relatively low oxygen content, has higher tensile strength. The effect of the lower oxygen content on the mechanical properties of this type of SiC fiber is thought to cause this phenomenon. Furthermore, it appears that as the oxygen content decreases, the percentage of SiC matrix within the SiC_xO_y matrix of the fiber increases, influencing fiber strength [9].

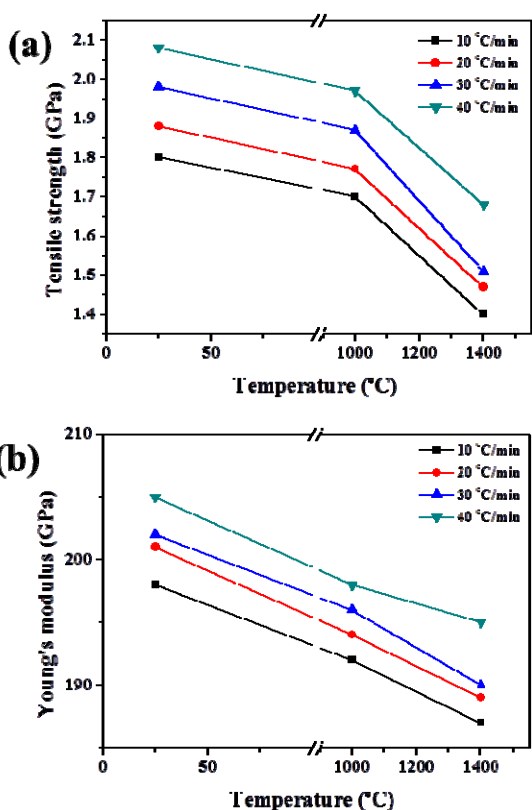


Fig. 8 (a) Tensile strength and (b) Young’s modulus of SiC fiber at different heating rates under ambient atmosphere at room temperature, 1000 °C, and 1400 °C.

Table 4 Average tensile strength and elasticity of SiC fiber with various heating rates at different temperatures (Unit: GPa)

Heating rate (°C/min)	Room temperature		1000 °C		1400 °C	
	Tensile strength	Elasticity	Tensile strength	Elasticity	Tensile strength	Elasticity
10	1.80	198	1.70	192	1.40	187
20	1.88	201	1.77	194	1.47	189
30	1.98	202	1.87	196	1.51	190
40	2.08	205	1.97	198	1.68	195

To evaluate the internal oxidation properties of the fiber, the weight analysis via TGA was performed on each of the produced fiber and is shown in Fig. 9. Internal oxidation analysis was performed up to 1100 °C, holding for 1 h at this final temperature. The cross-section of the fiber was then observed, as shown in Fig. 10, and the microstructure of the SiO₂ layer formed on the surface of SiC fiber was examined. Considering the TGA curve, an approximately 0.2%–0.5% weight reduction near the 200 °C range is determined to be the result of evaporation of H₂O on the fiber surface. An approximately 0.6%–1.5% weight reduction near 500 °C is believed to be due to emission of free carbon from the fiber. Subsequently, weight gaining is started from the approximately 800 °C due to the initiation of SiO₂ formation on the surface of the fiber, which continues up to 1100 °C. This results in the weight of the fiber showing a final yield of 98.8% at the slow heating rate of 10 °C/min, and yields of 99.32%, 99.34%, and 99.33%, for heating rates of 20, 30, and 40 °C/min, respectively. The largest yield difference is observed in SiC fiber with a heating rate of 10 °C/min. As seen in the internal oxidation evaluation in Fig. 10, the results of FE-SEM microstructure observations of the oxide layer reveal a 584 nm SiO₂ layer in the SiC fiber with a heating rate of 10 °C/min. For heating rates of 20, 30, and 40 °C/min, the results are 444, 325, and 304 nm, respectively. Both active and passive oxidation behavior theories exist to explain the internal oxidation properties of SiC fiber. In most cases, passive oxidation behavior tends to dominate [19]. Based on the evaluation of internal oxidation in Fig. 9 and the observations of SEM microstructure in Fig. 10, it is determined that thinner oxide layers are formed at higher heating rates and the properties of SiC fiber are not lost even at high temperatures.

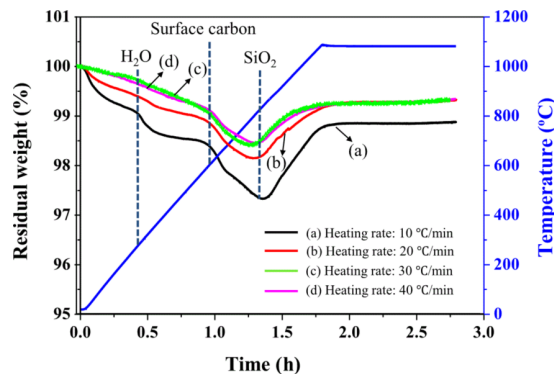


Fig. 9 Oxidation resistance test of after-pyrolysis SiC fiber at different heating rates using TGA measurement.

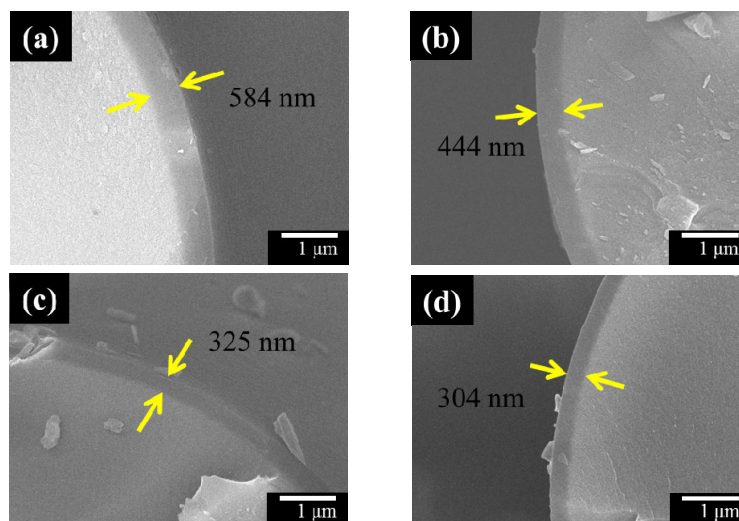


Fig. 10 Cross-section FE-SEM images of SiC fiber after oxidation resistance test at different heating rates: (a) 10 °C/min, (b) 20 °C/min, (c) 30 °C/min, and (d) 40 °C/min at 1100 °C.

The testing detailed in this study is based on the use of iodine vapor during the curing process, a critical process in production of SiC fiber. This method allows faster production without sacrificing the unique properties of SiC fiber and yields products with desirable properties. Further studies of high temperature heat treatment with higher heating rates are needed in the future.

4 Conclusions

In this study, we focused on rapid fabrication of high-yield and high-quality SiC fiber using a chemical vapor curing method incorporating iodine, which can achieve rapid curing at low temperatures, in lieu of a conventional thermal oxidation curing method. The SiC fiber cured by this method was produced at the heating rates of 10, 20, 30, and 40 °C/min. XRD patterns were used to confirm that the fiber was transformed to a zinc blende cubic structure through an amorphous silicon oxycarbide phase. SiC fiber produced with faster heating rates showed higher tensile strength and greater elasticity at room temperature, as well as at high temperatures. Consequently, it was determined that more rapid heating rates affect the mechanical properties of the fiber by decreasing its diameter and reducing the oxygen content by an increase in pyrolysis. During the evaluation of internal oxidation properties, a thin oxide layer was observed to form on the fiber surface, indicating desirable oxidation properties. Additional work is required to establish an

optimal processing for the chemical vapor curing. Studies are also needed on ultra-high temperature heat treatment to increase strength and allow for faster heating rates and the formation of fully crystalline SiC fiber.

Acknowledgements

The authors are appreciative for the financial support from the Korean Ministry of Knowledge and Economy, and the “Ceramic Fiber Commercialization Center” within the Korea Institute of Ceramic Engineering and Technology.

References

- [1] Liu HA, Balkus Jr. KJ. Electrospinning of beta silicon carbide nanofibers. *Mater Lett* 2009, **63**: 2361–2364.
- [2] Yu Y, Tai J, Tang X, *et al.* Continuous Si–C–O–Al fiber derived from aluminum-containing polycarbosilane precursor. *Composites Part A* 2008, **39**: 1101–1105.
- [3] Yu Y, Tang X. Ceramic precursor aluminum-containing polycarbosilane: Preparation and structure. *J Inorg Organomet P* 2009, **19**: 389–394.
- [4] Babonneau F. Synthesis and characterization of Si–Zr–C–O ceramics from polymer precursors. *J Eur Ceram Soc* 1991, **8**: 29–34.
- [5] Takeda M, Sakamoto J-i, Imai Y, *et al.* Thermal stability of the low-oxygen-content silicon carbide fiber, Hi-Nicalon™. *Compos Sci Technol* 1999, **59**: 813–819.
- [6] Ly HQ, Taylor R, Day RJ, *et al.* Conversion of polycarbosilane (PCS) to SiC-based ceramic: Part 1. Characterisation of PCS and curing products. *J Mater Sci* 2001, **36**: 4037–4043.
- [7] Kang P-H, Jeun J-P, Seo D-K, *et al.* Fabrication of SiC mat by radiation processing. *Radiat Phys Chem* 2009, **78**:

- 493–495.
- [8] Hong J, Cho K-Y, Shin D-G, *et al.* Low-temperature chemical vapour curing using iodine for fabrication of continuous silicon carbide fibers from low-molecular-weight polycarbosilane. *J Mater Chem A* 2014, **2**: 2781–2793.
- [9] William T, Batich CD, Sacks MD, *et al.* Polymer-derived silicon carbide fibers with low oxygen content and improved thermomechanical stability. *Compos Sci Technol* 1994, **51**: 145–159.
- [10] Shimoo T, Okamura K, Ito M, *et al.* High-temperature stability of low-oxygen silicon carbide fiber heat-treated under different atmosphere. *J Mater Sci* 2000, **35**: 3733–3739.
- [11] Bae J-C, Cho K-Y, Yoon D-H, *et al.* Highly efficient densification of carbon fiber-reinforced SiC-matrix composites by melting infiltration and pyrolysis using polycarbosilane. *Ceram Int* 2013, **39**: 5623–5629.
- [12] Kim T-E, Bae JC, Cho KY, *et al.* Thermal conducting behavior of composites of conjugated short fibrous-SiC web with different filler fraction. *J Korean Phys Soc* 2012, **49**: 549–555.
- [13] Kim T-E, Bae JC, Cho KY, *et al.* Fabrication of electrospun SiC fibers web/phenol resin composites for the application to high thermal conducting substrate. *J Nanosci Nanotechnol* 2013, **13**: 3307–3312.
- [14] Hasegawa Y. Synthesis of continuous silicon carbide fibre. *J Mater Sci* 1989, **24**: 1177–1190.
- [15] Xu T, Ma Q, Chen Z. Mechanical property and microstructure evolutions of C_v/SiOC composites with increasing annealing temperature in reduced pressure environment. *Ceram Int* 2012, **38**: 605–611.
- [16] Soraru GD, Babonneau F, Mackenzie JD. Structural evolutions from polycarbosilane to SiC ceramic. *J Mater Sci* 1990, **25**: 3886–3893.
- [17] Bunsell AR, Piant A. A review of the development of three generations of small diameter silicon carbide fibers. *J Mater Sci* 2006, **41**: 823–839.
- [18] Shimoo T, Toyoda F, Okamura K. Oxidation kinetics of low-oxygen silicon carbide fiber. *J Mater Sci* 2000, **35**: 3301–3306.
- [19] Shimoo T, Okamura K, Morisada Y. Active-to-passive oxidation transition for polycarbosilane-derived silicon carbide fibers heated in Ar–O₂ gas mixtures. *J Mater Sci* 2002, **37**: 1793–1800.

Open Access The articles published in this journal are distributed under the terms of the Creative Commons Attribution 4.0 International License (<http://creativecommons.org/licenses/by/4.0/>), which permits unrestricted use, distribution, and reproduction in any medium, provided you give appropriate credit to the original author(s) and the source, provide a link to the Creative Commons license, and indicate if changes were made.